Sensing of Transcription Factor through Controlled-Assembly of Metal Nanoparticles Modified with Segmented DNA Elements

Yen Nee Tan,[†] Xiaodi Su,[†,*] Yue Zhu,[‡] and Jim Yang Lee[‡]

[†]Institute of Material Research and Engineering, ASTAR (Agency for Science, Technology and Research), 3 Research Link, Singapore 117602 and [‡]Department of Chemical and Biomolecular Engineering, National University of Singapore, 10 Kent Ridge Crescent, Singapore 119260

ABSTRACT We have developed a unique metal nanoparticle (mNPs)-based assay to detect sequence-specific interactions between transcription factor and its corresponding DNA-binding elements. This assay exploits the interparticle-distance dependent optical properties of noble mNPs as sensing element and utilizes specific protein—DNA interactions to control the dispersion status of the mNPs. The assay involves two sets of double-stranded (ds)DNA modified-mNPs, each carrying a half site segment of a functional DNA sequence for the protein of interest. Each of these half sites is designed to contain a short complementary sticky end that introduces base-pairing forces to facilitate particle aggregation and to form a transient full dsDNA sequence. The detection of specific protein—DNA binding is founded on the premise that the mixture of these two sets of dsDNA—mNPs experiences a remarkable particle aggregation under certain salt conditions; whereas the aggregation can be retarded in the presence of a specific protein that binds and stabilizes the transient full dsDNA structure and therefore introduces steric protection forces between particles. We have demonstrated the concept using estrogen receptor α and its response elements, with gold and silver NPs as the sensing platform. UV—vis spectroscopy, transmission electron spectroscopy, and dynamic light scattering measurements were conducted to provide full characterization of the particle aggregation/dispersion mechanism. Differing from most of the mNP-based colorimetric sensors that are designed based on the analyte-induced aggregation mechanism, current protein binding-stabilization sensing strategy reduces the false signals caused by unrelated particle destabilizing effects. It is expected that this assay principle can be directed toward other transcription factors by simply changing the recognition sequence to form different segmented dsDNA—mNP constructs.

KEYWORDS: gold nanoparticles · silver nanoparticles · colorimetric sensing assay · transcription factors · protein—DNA binding · estrogen receptors · estrogen response elements

Noble metal nanoparticles (mNPs) have unique optical properties arising from their ability to support a localized surface plasmon resonance (LSPR).[1] These optical properties are determined by the material properties of the mNPs such as chemical composition, particle shape, size (or spacing), and dielectric constant of the surrounding medium. One powerful and simple way to use mNPs for biosensing is to construct colorimetric assays that exploit the particle size (or interparticle spacing)-determined LSPR properties and solution color as sensing elements.[2−4] Biomolecular interactions and biological processes can be detected on the basis of their modulation of the mNPs' dispersion and aggregation status. Changing of interparticle distance will change the particle−particle plasmonic coupling and the aggregate scattering that are measurable by a distinct LSPR spectrum shift and/or particle solution color changes.

Mirkin and co-workers reported the first colorimetric assay for the detection of nucleic acid hybridization[5] upon their development of single-stranded (ss)DNA-conjugated gold nanoparticles (AuNPs) that exhibited strong color change and LSPR red shift in the presence of target DNA. Since then, the design and preparation of mNPs conjugates with a variety of receptors (*e.g.*, aptamers,[6,7] peptides,[8−11] antibodies,[12−14] DNA,[15−17] *etc.*) have attracted great attention. Development of more generic, robust, and reliable (less false positive results) colorimetric assays has formed an important branch of research. The use of DNA−mNPs conjugates as colorimetric probes has been extended from measuring nucleic acids hybridization[5,15−17] to detecting various DNA binders (*e.g.*, small molecules,[18−20] drugs,[21,22] metal ions,[23−27] *etc.*) and to monitoring different DNA-related enzymatic reactions.[28−32] In most of the assays for DNA hybridization and for DNA binders, DNA−mNPs conjugates are assembled into aggregates through formation of interparticle-molecular linkers such as DNA−duplexes, DNA−triplexes, DNA−small molecule complexes, and DNA−metal−DNA coordination complexes. UV−vis melting temperature measurements are often used to detect

*Address correspondence to xd-su@imre.a-star.edu.sg.

Received for review April 30, 2010 and accepted August 05, 2010.

Published online August 12, 2010. 10.1021/nn100943d

single-base-mismatch in DNA duplex[5] and to determine the binding strength of DNA binders.[18,20−23,26] In DNA-related enzymatic assays, for example, endonucleases cleavage of DNA, dissociation of DNA-linked particle aggregates in the presence of endonucleases provides the measures of enzymatic activity and/or inhibition.[28−31] Despite the wide range applications of DNA−mNPs conjugates, their utilities for detecting DNA binding proteins, another category of DNA binder, have been less well demonstrated.[7,33]

DNA-binding proteins (*e.g.*, transcription factors, polymerases, and nucleases) are proteins that contain DNA-binding domains and thus have a specific or general affinity for either single- or double-stranded DNA. Interactions between these proteins and DNA play critical roles in many biological processes. Sequence-specific DNA-binding proteins, such as transcription factors, modulate the process of gene transcription by binding to a specific double-stranded (ds)DNA sequence. It is crucial to develop reliable techniques capable of measuring transcription factor−DNA interactions with high sequence specificity. Most recently, an AuNPs-based assay for *lac* repressor (a most extensively studied transcription factor) has been reported.[33] This assay exploited (ds) *lac* operator-conjugated AuNPs as sensing probes. *Lac* repressor (protein) and *lac* operator (DNA) binding was monitored based on the facts that *lac* repressor binds with *lac* operator as homodimers, where the two homodimers join at the C-terminus to form a tetramer. The divalent binding property enables the *lac* repressor protein to serve as a bridge to connect the *lac* operator conjugated DNA−AuNPs to form particle aggregates. Unlike the aforementioned assays for DNA binders,[18−32] including DNA-binding protein for enzymatic reaction,[28−32] that rely on the formation/dissociation of interparticle DNA duplex linkers, the dimer−dimer interface connection of lac repressor are responsible for the formation of AuNPs aggregates. As such no target (protein) recognition of DNA linkers embedded inside the network particle aggregates is needed, which often leads to slow colorimetric response due to the poor accessibility.[32] Similarly, in another assay for protein (platelet-derived growth factors) and its DNA aptamers, the fact that the aptamer binds to the protein in a 2:1 fashion is exploited to aggregate the particles.[7] While the use of divalent binding property of a protein to design protein−DNA binding assay is innovative, it may exhibit a limitation to the generality for other proteins that do not have such a property.

In this study, we have developed a mNPs-based protein−DNA binding assay that has no such limitation, owing to an elegant design of double-stranded (ds)DNA−mNPs conjugates and therefore a more generic aggregation principle. Particularly this assay involves two sets of dsDNA−mNPs conjugates, each carrying a half site segment of a functional dsDNA sequence for the protein of interest. These dsDNA half sites are designed to contain a sticky end of a small number of nucleotides that are complementary to each other, introducing a tendency to form a transient full dsDNA sequence for protein recognition and a driving force to facilitate particle aggregation in the presence of salt ions. The detection of specific protein−DNA binding is based on the observation that the mixture of these two sets of dsDNA−mNPs experiences a remarkable particle aggregation under certain salt conditions; but the aggregation can be retarded in the presence of protein due presumably to the binding of the protein to the transient full dsDNA sequence that can insert steric protection forces between the particles and stabilize the transient structure. We have demonstrated the concept using estrogen receptor α and its response elements, with gold and silver NPs as the sensing platform. UV−vis spectroscopy, transmission electron microscopy (TEM), and dynamic light scattering (DLS) measurements were conducted to provide full characterization of the particle aggregation/dispersion mechanism. This "light off" sensing strategy using analyte as a stabilizer to prevent particle aggregation,[8] avoids the false positive results as often seen in the "light on" assays where analyte binding causes particles to aggregate. It is expected that this assay principle can be directed toward other transcription factors by simply changing the recognition sequences used to form segmented dsDNA−mNPs constructs.

TABLE 1. Estrogen Response Elements (ERE) Sequences

names (denoted as)	oligonucleotide sequences
sense strand of consensus ERE (v)	5′-GTCCAAAGTCAGGTCACAGTGACCTGATCAAAGT-3′
(ds) ERE half site 1 (v1)	5′-HS$(CH_2)_6$-GTCCAAAGTCAGGTCACAG-3′
	3′-CAGGTTTCAGTCCAGT-5′
(ds) ERE half site 2 (v2)	5′-HS$(CH_2)_6$-ACTTTGATCAGGTCACTG-3′
	3′-TGAAACTAGTCCAGT-5′
sense strand of scrambled DNA (s)	5′-GTCCAAAGTCA*ATCGC*CAG*CACGA*TGATCAAAGT-3′
(ds) scrambled half site 1 (s1)	5′-HS$(CH_2)_6$-GTCCAAAGTCA*ATCGC*CAG-3′
	3′-CAGGTTTCAGT*TAGCC*-5
(ds) scrambled half site 2 (s2)	5′-HS$(CH_2)_6$-ACTTTGATCA*TCGTG*CTG-3′
	3′-TGAAACTAGT*AGCAC*-5′

RESULT AND DISCUSSION

Preparation of Segmented dsDNA−mNPs Conjugates and Stability Test. Estrogen receptor α (ERα) is a nuclear receptor that regulates estrogen gene transcription by binding to its response elements (EREs). The consensus ERE from vitellogenin A2 gene (vit ERE) is a 34 bp double-stranded DNA that contains a core sequence (5′-GGTCAnnnTGACC-3′, n: spacer nucleotides) for ERα protein to bind at a high affinity (the sense sequence of vit ERE is shown in Table 1). As shown in Figure 1, the consensus vit dsERE was split into two half ERE segments (denoted as v1 and v2, respectively) with a 3-bases complementary sticky end. AuNPs were func-

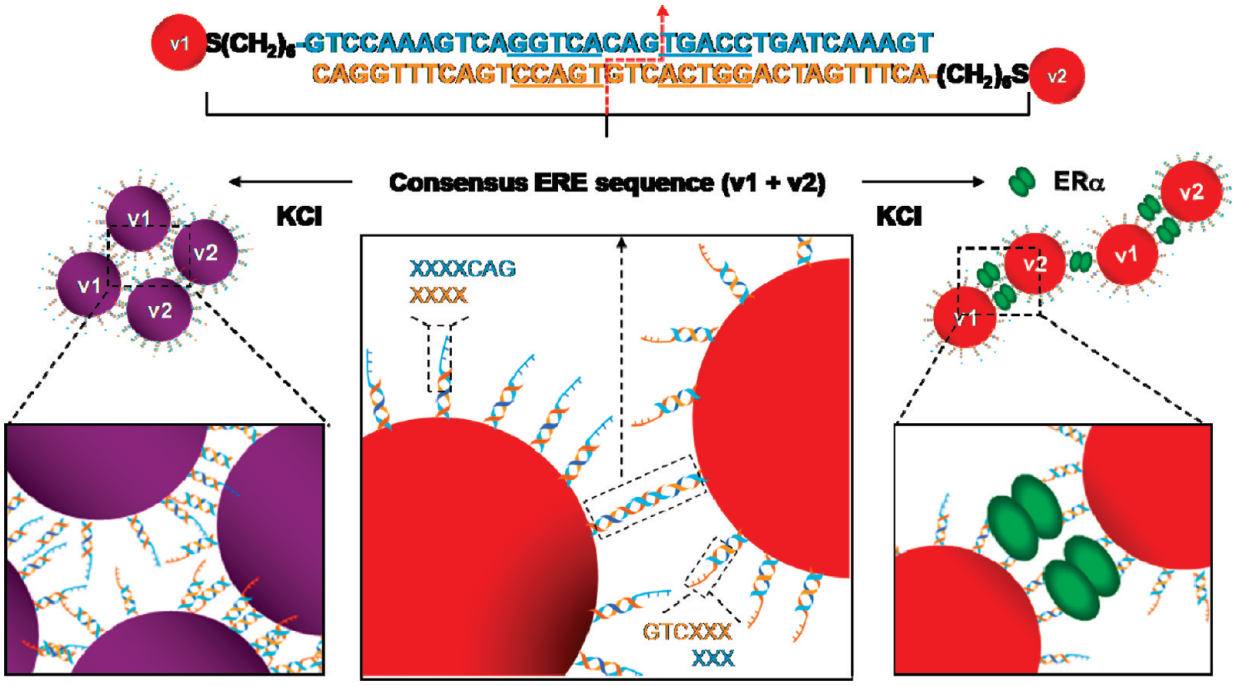

Figure 1. Schematic illustration of sensing principle. Two sets of gold nanoparticles (AuNPs) each is modified with a half ERE segment (v1 and v2) containing 3-bases complementary sticky ends. These particles, when mixed together at 1:1 molar ratio, have a tendency to aggregate through Watson−Crick base-pairing force (middle). The addition of KCl screens the charge repulsion between DNA−AuNPs and promotes base paring, resulting in rapid particle aggregation and solution color change from red to purple (left). In the presence of ERα, the binding of the protein to the transient full ERE sequence between AuNPs exerts steric force to stabilize the AuNPs and thus solution color remains red (right).

tionalized with the thiolated v1 and v2 sequences (see Table 1) to form v1−AuNPs and v2−AuNPs conjugates, respectively. These as-prepared AuNPs conjugates (in 0.1 M PBS) were red in color and showed no traces of aggregation even in ERα binding buffers, which contains 0.1 M PBS, 25 or 50 mM KCl, 0.01 mM EDTA, 0.2 mM DTT, and 1% glycerol, for at least 20 min (see TEM images in Figure S1A, Supporting Information). The localized surface plasmon resonance (LSPR) spectrum of these conjugates exhibits a sharp peak at 520 nm in all tested buffer conditions, that is, 0.1 M PBS (no KCl), and protein binding buffer containing 25 or 50 mM KCl (curves a, Figure 2A−C). However, remarkable particle aggregation was observed when two sets of complementary v1−AuNPs and v2−AuNPs conjugates were mixed at a 1:1 ratio under the same buffer conditions, characterized as a LSPR peak shift to a longer wavelength with band broadening (curves b, Figure 2A−C) and solution color change from red to purple (insets of Figure 2, left). The TEM image for the condition of 25 mM KCl (Figure S1B, Supporting Information) provides a visual evidence of the aggregation. To further evince that the LSPR shift and solution color change are related to the particle aggregation, we have used the dynamic light scattering (DLS) technique to measure the hydrodynamic diameter (D_h) of the stable (dispersed) v1−AuNPs conjugate alone and the complementary mixture of v1−AuNPs and v2−AuNPs. Results (Figure 2 right panels) show that the particle sizes (see average effective diameter) of the complementary conjugates mixture are much larger than those of the dispersed v1−AuNPs (D_h = 34.2 ± 0.2 nm) (size distribution graph not shown), and the size increases with the increase of KCl concentration. The salt concentration-dependent particle aggregation suggests that the charge screening (by salt ions) causes the AuNPs to lose their electrostatic stabilization forces. Furthermore, it was found that the complementary set of v1−AuNPs and v2−AuNPs mixture also underwent aggressive aggregation in buffer condition without KCl after exposure to 0.1 M PBS for 20 min (curve c, Figure 2A). This observation imparts that the complementary sticky ends of the v1- and v2-sequences introduce base-pairing forces to facilitate salt-induced particle aggregation. To prove this hypothesis, we have conducted a control experiment with a mixture of dsDNA−AuNPs conjugates that carry noncomplementary dangling ends, that is, v1−AuNPs with s1−AuNPs (s1 is a half site of a non-ERα binding DNA, in which the ERE site is scrambled; s1 has a noncomplementary dangling end with v1 sequence. The sequences of the two half sites of scrambled DNA, that is, s1 and s2, are shown in Table 1). The UV−vis spectrum of the v1−AuNPs and s1−AuNPs mixture (1:1 ratio) measured after 20 min of incubation in the 25 mM KCl-containing protein binding buffer overlapped with the stable v1−AuNPs conjugates alone under the same buffer condition (Figure S2A, Supporting Information). This result indicates that complementary sticky ends are essential to initiate aggregation/instability to the particle mixture. TEM im-

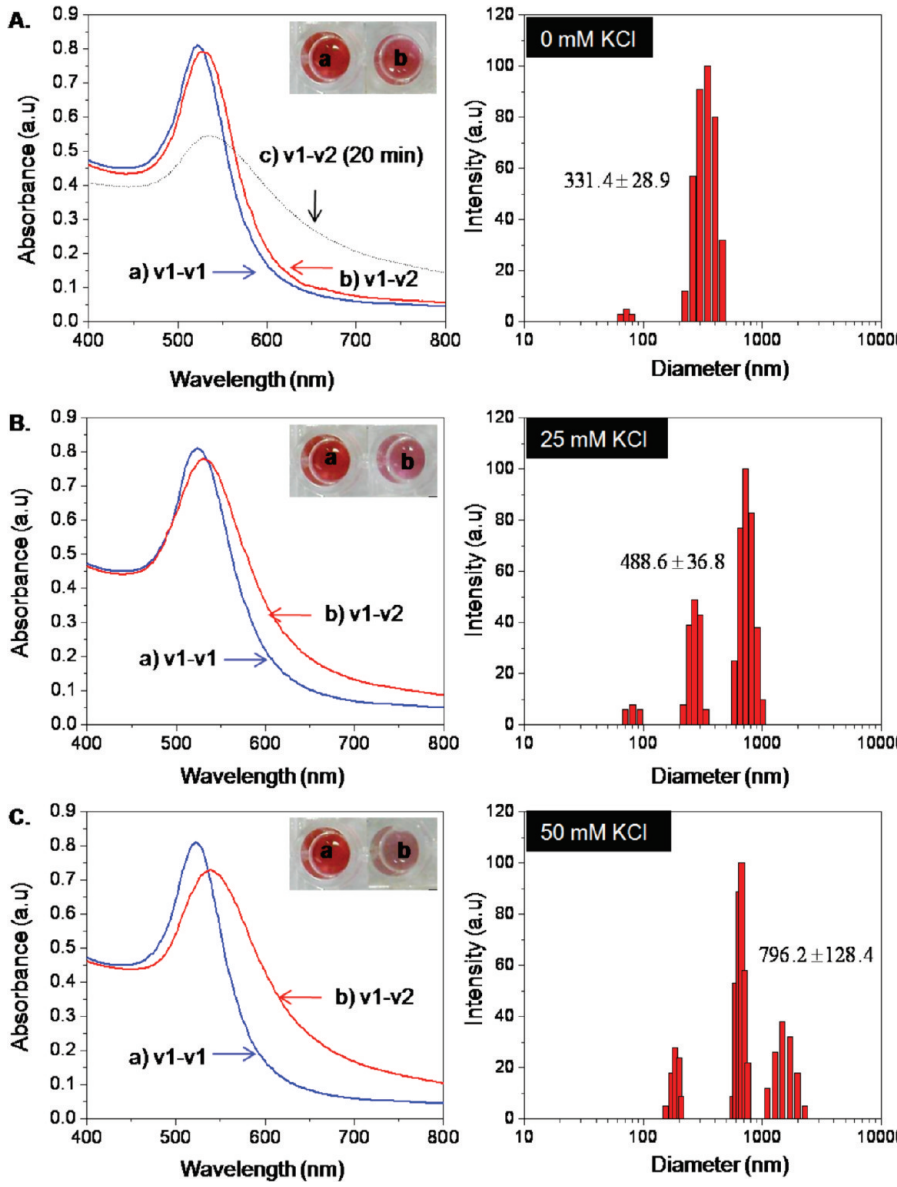

Figure 2. (Left) UV−vis spectra of v1−AuNPs alone (curves a) and complementary v1−v2 AuNPs mixture (1:1 ratio) (curves b) in protein binding buffer of 0.1 M PBS containing (A) 0, (B) 25, and (C) 50 mM KCl, and 0.1 mM EDTA, 0.2 mM DTT, and 1% of glycerol. All the spectra (curves a and b) and color photographs of particle solution (insets) were taken at 1 min upon addition of salt buffer except that curve c in Figure 2A was taken after 20 min of incubation. (Right) Size distribution and calculated average hydrodynamic diameter (measured by DLS) of the complementary v1−v2 AuNPs mixture after 10 min of incubation.

ages taken for the noncomplementary v1−s1 and complementary s1−s2 mixtures of conjugates further confirmed the differential particle stability (Figure S2, Supporting Information). On the basis of the above results, we infer that it is the hybridization tendency of the complementary nucleotides that brings the particles in close vicinity to assist in the salt-induced aggregation. As the melting temperature of the complementary nucleotides (−CAG−) used in this study is only 10 °C, the three DNA base pairs are not strong enough to hold the 34 bp transient full vit ERE−AuNPs structures for a long period of time at room temperature. Furthermore, when the two particles are in close enough proximity, the charge screening effects by salt ions is amplified, leading to a more aggressive particle aggregation as time elapsed.

To further understand the condition for the complementary conjugates to form aggregates, particularly the DNA length effect, two shorter (15 and 25 bp) and one longer (45 bp) length of EREs were involved. Using a similar protocol for the previous 34 bp ERE, each of these EREs was split into two half segments with a complementary sticky end (see sequences in Table S1, Supporting Information), and were conjugated onto AuNPs to form v1$_{_xbp}$−AuNPs and v2$_{_xbp}$−AuNPs (x = 15, 25, 34, and 45), respectively. The UV−vis spectroscopy, DLS, and solution color change results (Figure 3) revealed that large aggregates were formed only in

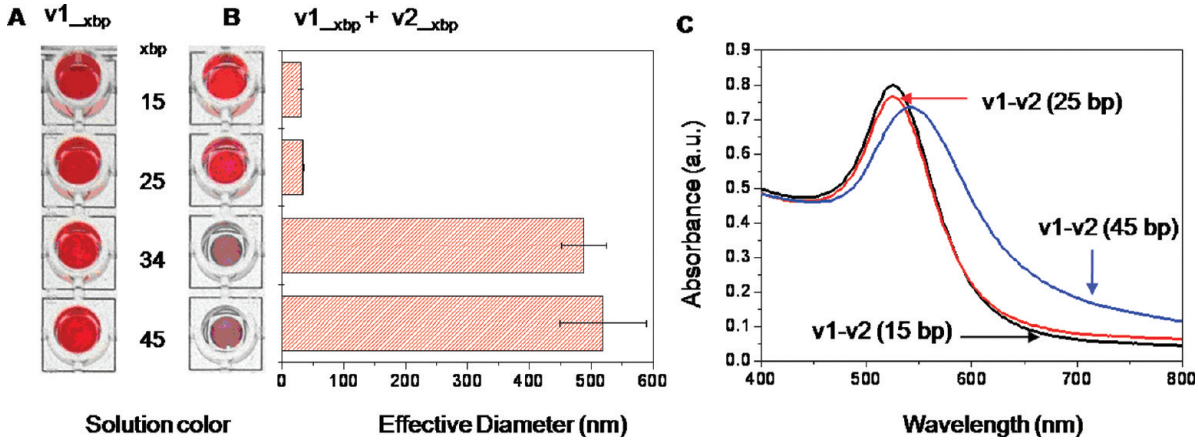

Figure 3. Length effects of dsDNA on AuNPs aggregate formation. Color photograph of (A) v1$_{_xbp}$−AuNPs and (B) (left) complementary v1$_{_xbp}$−v2$_{_xbp}$ AuNPs mixture, in protein binding buffer containing 0.1 M PBS, 25 mM KCl, 0.1 mM EDTA, 0.2 mM DTT, and 1% of glycerol. (Right) Aggregates sizes of particles (measured as effective hydrodynamic diameter by DLS) formed in the complementary mixture of AuNPs conjugates modified with different lengths of dsDNA (x = 15, 25, 34, and 45 bp). DLS data and color photograph of the AuNPs were taken at 10 min upon addition of salt buffer. (C) UV−vis spectra of the complementary v1$_{_xbp}$−v2$_{_xbp}$ AuNPs taken at 1 min upon mixing in the 25 mM KCl-containing protein binding buffer.

the complementary mixture of AuNPs conjugates modified with the longer 34 bp and 45 bp ERE segments (redshift of LSPR spectrum, large D_h of 488.6 ± 36.8 and 548.4 ± 56.2 nm, respectively, and purple color solutions). For those with shorter ERE (15 and 25 bp) segments, the D_h (32.4 ± 0.2 nm) remain similar to the v1−AuNPs alone (34.2 ± 0.2 nm) and no LSPR shift and solution color change are observed. We believe the longer dsDNA segments are essential to promote base pairing between the sticky end sequences that are far away (extended by the rigid dsDNA structure) from the particle interfaces, and thus lead to a faster aggregation.[34] When the dsDNA segments are too short, base paring is prohibited due to the inaccessibility of the sticky ends.

In the next section we will show that the instability of the complementary particles mixture is essential to the design of current protein binding assay. Thus the v1$_{_xbp}$−v2$_{_xbp}$ AuNPs prepared with the shorter segments (x = 15 bp and 25 bp) are not suitable for the protein binding assay, because the mixture of complementary particles conjugates shows no sign of aggregation.

Protein Sensing Using Segmented dsDNA−AuNPs Conjugates. Previously we have shown that the aggregation of v1−v2 AuNPs mixture was driven by the synergic effects of base-pairing between the complementary sticky ends of dsDNA half sites and charge screening by salt ions. Herein, we demonstrated that the instability of the complementary mixture in KCl-containing PBS buffer can be used to detect sequence-specific protein binding event, using the 34 bp consensus ERE sequence as an example. In Figure 2B, we have shown that the complementary mixture of v1−v2 AuNPs underwent remarkable particle aggregation in the protein binding buffer containing 25 mM KCl (curve b) at 1 min incubation, as revealed by a red shift in LSPR peak to 535 nm. In Figure 4A, we further observed that this mixture (without protein) aggregated more intensively at 20 min incubation, characterized by a larger peak shift to

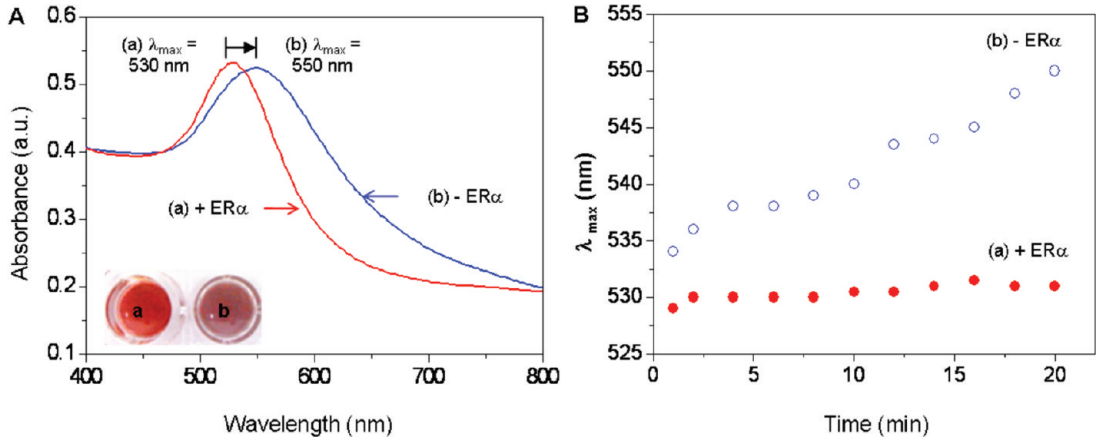

Figure 4. (A) UV−vis spectra and (B) kinetic of LSPR peak (λ_{max}) shift of the complementary v1−v2 AuNPs mixture (1:1 ratio) in the 25 mM KCl-containing protein binding buffer (0.1 M PBS, 25 mM KCl, 0.1 mM EDTA, 0.2 mM DTT and 1% of glycerol) with ERα (curve a and sphere) and without ERα (curve b, hollow sphere). UV−vis spectra and color photographs (inset of A) of the AuNPs mixture were taken at 20 min upon addition of salt buffer.

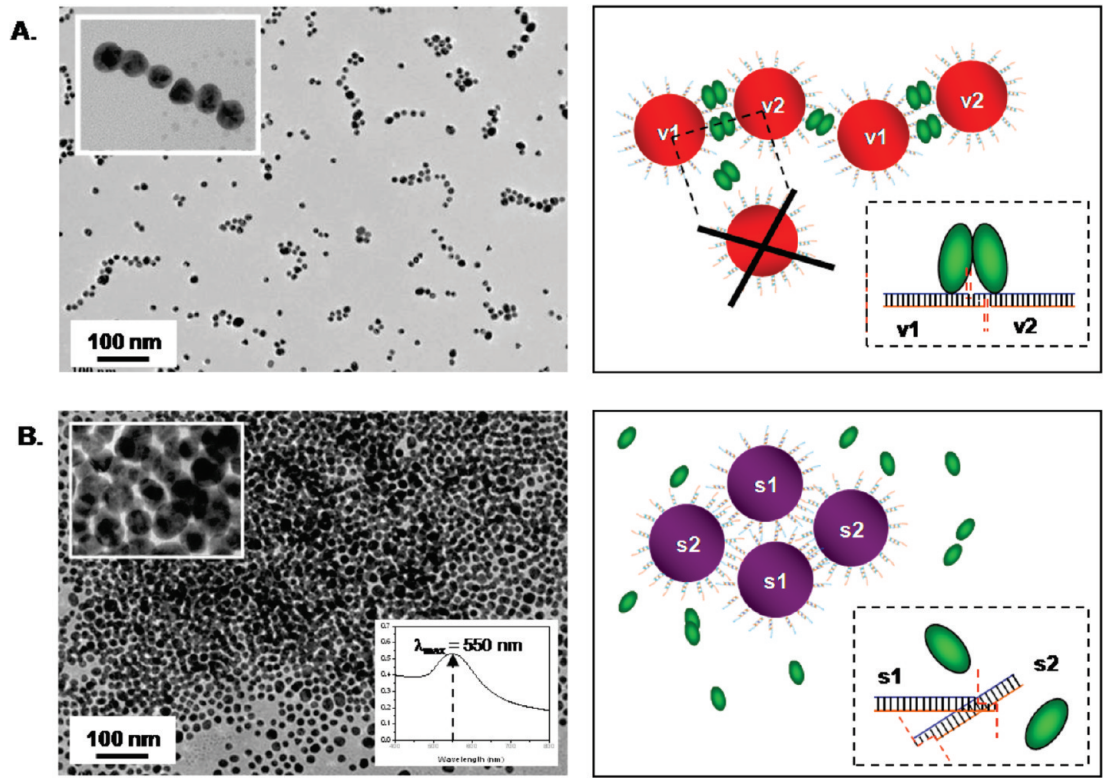

Figure 5. TEM images (left) and corresponding particle aggregation mechanism (right) for the complementary mixture of (A) v1−AuNPs and v2−AuNPs (1:1 ratio) and (B) s1−AuNPs and s2−AuNPs (1:1 ratio), in the protein binding buffer containing 0.1 M PBS, 25 mM KCl, 0.1 mM EDTA, 0.2 mM DTT and 1% of glycerol, in the presence of ERα (100 nM, final concentration). All the TEM images were sampled after 20 min of reaction with ERα in salt buffer.

550 nm (curve b). In contrast, when ERE-binding protein (*i.e.*, ERα) was added, only a small shift in peak position (λ_{max} = 530 nm) was observed at the same time frame (20 min) under the same salt condition (curve a, Figure 4A). The suspension with ERα kept a distinct red color (inset a of Figure 4A). The time course of the particle aggregation (shown as a function of peak wavelength shift over time in Figure 4B) for the mixture of v1−v2 AuNPs with and without ERα further confirms the distinctive stabilization effect of ERα throughout the tested period of 20 min. The same protein binding experiment was conducted for the AuNPs modified with the complementary half site of 45 bp ERE ($v1_{\_45bp}$−$v2_{\_45bp}$ AuNPs). Similar stabilization effects were also observed in the presence of ERα (Figure S3, Supporting Information). We have speculated it is the specific binding of ERα to its recognizable transient full vit ERE sequence (formed through initial base-pairing between the complementary v1 and v2 half sites) that is responsible for the retainable stability of particle mixture. The formation of v1−AuNPs/ERα/v2−AuNPs complex stabilizes the transient full ERE and inserts a sufficient steric barrier between the particles to prevent them from further aggregation by charge screening. The TEM image of the complementary mixture of v1−v2 AuNPs in the presence of ERα shows no large aggregates formation (Figure 5A) but a few strands of short linear particle assemblies (inset of Figure 5A and more TEM images in Figure S4, Supporting Information) formed in the stable particle mixtures. This is similar to the report by Kim *et al.* that a short linear connection of AuNPs in their system did not bring about a significant instability of nanoparticles.[35] The most probable reason for the linear assemblies as observed in our system is that the adhered proteins between the two complementary AuNP conjugates may prohibit other AuNP conjugates from approaching in oxygonal directions due to steric hindrance. Nonetheless it is more energetically favorable for the incoming AuNP conjugates to attach at the opposite site of the protein-adsorbed surface because of less space constraint as illustrated in Figure 5A (see schematic diagram). DLS results further confirmed the formation of small linear assemblies of the complementary v1−AuNPs and v2−AuNPs mixture with ERα. The average hydrodynamic diameter of this mixture is 200 ± 8.9 nm, which is larger than the dispersed v1−AuNPs conjugate (34.2 ± 0.2 nm) but smaller than the "huge" aggregates of the complementary mixture of v1−v2 AuNPs without ERα under same buffer conditions (488.6 ± 36.8 nm).

To verify that the sequence-specific protein−DNA binding event is responsible for the particle stabilization, we have conducted two control experiments that involved (1) the scrambled DNA (non-ERα binding sequence) and (2) an irrelevant protein (bovine serum albumin, BSA) respectively. In the first control experi-

ment, we functionalized the AuNPs with the two half sites s1 and s2 (each contains a 3-bases sticky end) of the dsDNA sequence in which the ERα binding site is scrambled (sequence of the scrambled DNA and its half-site segments are shown in Table 1). We then mixed them together (1:1 molar ratio) and tested their stability in the presence of 100 nM of ERα. Both the TEM image (Figure 5B) and the corresponding UV−vis spectra (red shift in LSPR peak to 550 nm, inset of Figure 5B) show that the complementary mixture of s1−s2 AuNPs underwent extensive aggregation, similar to the case where no ERα was added (Figure S2B, Supporting Information). This indicates that no protein binding to DNA has occurred. Because of the lack of steric protection by protein adsorption to the transient dsDNA−AuNPs structure to counteract with the charge screening process by salt ions, the particles are largely aggregated (see schematic illustration in Figure 5B). In the second negative control experiment, the stability of the complementary mixture of v1−v2 AuNPs was tested in the presence of an irrelevant protein (*i.e.*, BSA in this case) that has no specific binding to ERE sequence. The particle mixture in the presence of BSA experienced a similar aggregation profile in salt solution as observed for that without protein added (Figure S5, Supporting Information), showing that no protein−DNA binding event has happened. With the results of these negative control experiments, we have concluded that it is the sequence-specific protein−DNA (ERα−ERE) binding event that is responsible for the higher stability of the complementary dsDNA−AuNPs mixtures with specially designed segmented protein binding sequences.

Detection Sensitivity of Protein−DNA Binding Assay with Optimized Buffer Conditions. In the stability tests for the dsDNA−AuNPs conjugate mixtures (Figure 2), we have shown that in protein binding buffer containing a higher concentration of KCl (50 mM), the complementary mixture of v1−v2 AuNPs mixture exhibits a higher instability, more easily detectable in 1 min upon addition of the buffer solution. The higher instability of particle mixture would be appreciated for a rapid detection of protein in the binding-stimulated stabilization assay. Indeed, in the protein binding experiment conducted previously under a lower salt (25 mM KCl) condition (Figure 4), a longer incubation time (up to 20 min) was desirable for a more obvious observation of the stabilization effect. In the next experiments, taking the advantage of the higher instability in the 50 mM KCl-containing buffer, we have tested the ERα binding in 1 min incubation for a range of protein concentration (0−200 nM) (Figure 6A). Solid−liquid phase SPR experiments were conducted to show that 50 mM KCl is an optimal condition to ensure a higher efficiency in ERα−ERE binding, relative to the 25 mM KCl, because it is closer to the physiological salt concentration[36−38] (Figure S6, Supporting Information). Results in Figure 6A shows that ERα effectively retarded the aggregation

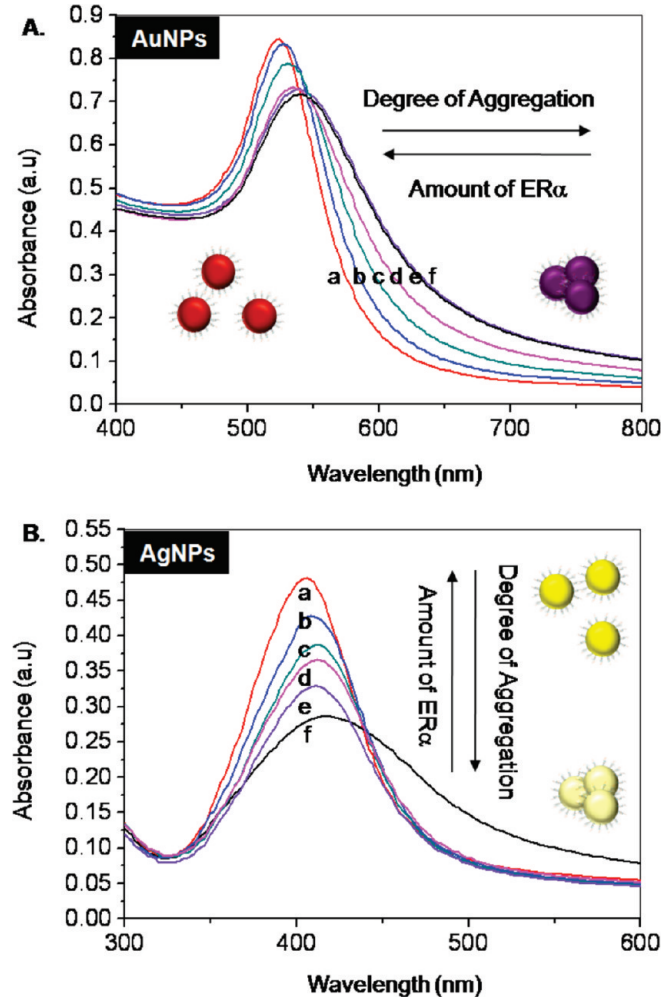

Figure 6. UV−vis spectra of the complementary mixture of v1−v2 particles conjugates for the (A) AuNPs and (B) AgNPs with (b) 200, (c) 100, (d) 50, (e) 25, and (f) 0 nM of ERα in the 50 mM KCl-containing protein binding buffer (0.1 M PBS, 50 mM KCl, 0.1 mM EDTA, 0.2 mM DTT, and 1% of glycerol). UV−vis spectra of stable v1−mNPs conjugates under the same buffer conditions (curve a) is shown as a reference. All the spectra were taken at 1 min upon addition of ERα-containing salt buffer.

of the complementary mixture of v1−v2 AuNPs. The degree of stabilization is increased with the increase of protein concentration. For example, only a slight shift in the UV−vis spectrum is observed for the v1−v2 AuNPs mixture in the presence of 200 nM ERα (the highest concentration tested) (curve b) relative to a stable v1−AuNPs conjugate (curve a) at $t = 1$ min. In such a short incubation time, ERα down to 50 nM can be detected by a remarkable stabilization effect. Both the improved ERα−ERE binding efficiency and the larger shift in LSPR peak (relative to a stable v1−AuNPs at $\lambda_{max\_v1} = 520$ nm) for the v1−v2 AuNPs mixture in the 50 mM KCl-containing buffer (*i.e.*, $\lambda_{max\_v1v2} = 545$ nm, Figure 2C) are attributable to the effective detection of low concentration of ERα in a short incubation time. Indeed, when the comparison is made for the 1 min binding of 100 nM ERα in the 25 mM KCl- (Figure 4B) and 50 mM KCl-containing buffer solutions, we found that

the recoveries of the peak wavelength (*i.e.*, $\Delta\lambda_{max} = \lambda_{max\_v1v2} - \lambda_{max\_v1v2\text{-}ER\alpha}$) for the former and latter conditions are 5 and 15 nm, respectively. The larger degree of stabilization under the 50 mM KCl condition affirms the solid−liquid phase SPR result that ERα binding is more effective when the condition is closer to physiological conditions. All these results suggest that the less stable the v1−v2 AuNPs mixture in (high) salt solution is, the faster is the aggregation and the more significant is the stabilization effects of ERα that can be detected in short assay time. The protein binding-particle stabilization mechanism used in this assay design also reduces the risk of getting a false positive caused by unrelated particle destabilizing effects.

Proof-of-Concept Using Silver Nanoparticles. Silver nanoparticles (AgNPs) are known to have a higher extinction coefficient[15,37] and to be more sensitive in responding to the changes in stabilization forces.[40,41] These properties have rendered AgNPs a more sensitive platform for use in colorimetric assays.[15,39−41] In this study, segmented DNA-conjugated AgNPs were prepared and were tested for ERα binding to confirm the sensing strategy and to demonstrate the utility of AgNPs in this instance. The dsDNA−AgNPs stability test shows that the mixture of the complementary v1−v2 AgNPs conjugates (no ERα added) aggregated drastically in the 50 mM KCl-containing protein binding buffer solution (curve f, Figure 6B). A remarkable dampening of the UV−vis spectra of AgNPs, in particular, drop in absorbance from its original peak wavelength of 400 nm (curve a, Figure 6B) was observed, accompanied by an intense color change from yellow to pale brown. The binding of ERα (curve b−e, Figure 6B), on the other hand, retarded the particle aggregation effectively in an ERα concentration-dependent manner. Negative control experiments involving non-ERE−AgNPs conjugates (*i.e.*, s1−s2 AgNPs) and irrelevant proteins (*e.g.*, BSA) were conducted to further confirm the sensing principle (data not shown). We believe it is again the steric protection forces exerted by the large protein molecules upon formation of v1−AgNPs/ERα/v2−AgNPs complex that prevent the particle conjugates from aggregation. The detection limit of ERα binding using the AgNPs assembly platform is 25 nM, which is lower than that using the AuNPs sensing probe under the same buffer conditions (50 mM KCl) and assay time (t = 1 min). We thus infer that AgNPs is a more sensitive platform to be used in our sensing strategy for protein detection.

CONCLUSION

We have developed a colorimetric sensing strategy for measuring sequence specific interactions between proteins and dsDNA. The key of the sensing design lies in the design of dsDNA−mNPs conjugates with segmented protein binding sequences carrying sticky ends. This allows for an innovative sensing principle where proteins serve as a stabilizer to retard the aggregation of the complementary dsDNA−mNPs mixture that is driven by synergic effects of base-pairing (between complementary overhangs of dsDNA) and charge screening (by salt ions). We have validated the assay principle with gold NPs and have determined the suitable length of DNA and buffer conditions to be used in this assay. We have also extended the assay using silver NPs upon successful preparation of the conjugates, and have proven that silver NPs is a more sensitive platform in this application. Compared to the other assays for DNA binders that rely solely on the formation of interparticle DNA duplex linkers to aggregate the particles, the use of synergic aggregation forces and the steric stabilization makes the sensing process faster. Unlike those assays that use analyte-induced particle aggregation ("light on" assay), current protein binding-stabilization mechanism ("light-off" assay) reduces the risk of getting false positive results caused by unrelated particle destabilizing effects. This assay involves no intensive interparticle hybridization and requires no careful monitoring of melting (dissociation) behavior that is often used in other DNA binder assays. Besides, the protein binding-controlled stable linear particle assemblies may provide an additional value for the research of biomolecular-induced inorganic nanoassembly.

METHODS

Materials and Instrumentation. Hydrogen tetrachloroaurate (III) ($HAuCl_4 \cdot 3H_2O$, 99.9%), silver nitrate ($AgNO_3$, 99.9%), and sodium borohydride ($NaBH_4$, 98%) were purchased from Sigma-Aldrich. Sodium citrate dihydrate ($Na_3C_6H_5O_7 \cdot 2H_2O$, 99%) was obtained from Alfa Aesar. Purified recombinant human estrogen receptor alpha (ERα) was supplied by PanVera Corporation (Madison, WI). Estrogen response elements (ERE) used in this study (Table 1) were synthesized by Sigma-Proligo (Singapore).

All chemicals and materials were used as received without further purification. Ultrapure water (18MΩ, prepared from Millipore Elix 3 purification system) was used as solvent unless indicated otherwise. A TECAN infinite M200 plate reader (Tecan Trading AG, Switzerland) was used to measure the UV−vis adsorption spectrum, and 96-well clear flat-bottom UV-transparent microplates (Corning Incorporated, USA) were used as reaction carrier. Dynamic light scattering (DLS) measurement was conducted in the Brookhaven 90PLUS nanoparticles size analyzer using a 50 μL disposable cell as the solution carrier. JEOL 2100 transmission electron microscope (TEM) operating at 200 kV was used for gold nanoparticles (AuNPs) imaging. All the samples for microscopy were prepared by dispensing 10 μL of the nanoparticle solution onto a 3 mm carbon-coated copper grid, followed by drying in vacuum at room temperature.

Synthesis of Gold Nanoparticles (AuNPs). AuNPs (*ca.* 13 nm in diameter) were synthesized by sodium citrate reduction of $HAuCl_4$. Briefly, an aqueous solution of sodium citrate (5 mL, 38.8 mM) was added rapidly to a boiling solution of $HAuCl_4$ (50 mL, 1 mM) under reflux and vigorous stirring for 15 min. The color of the solution changed from pale yellow to deep red. Stirring was con-

tinued for an additional 15 min after removing the heating mantle and allowed to cool to room temperature for use.

Synthesis of Silver Nanoparticles (AgNPs). AgNPs (*ca.* 40 nm in diameter) were synthesized by seed-mediated growth method. A mixture of $AgNO_3$ (1 mL, 20 mM), sodium citrate (0.8 mL, 80 mM) and 17.8 mL of ultrapure water were brought to reflux for 1 min. An aqueous solution of sodium borohydride (0.4 mL, 0.1 mM) was added dropwise to the solution mixture with vigorous stirring. The formation of AgNPs seeds was indicated by the solution color change from colorless to yellow. The AgNPs seeds were further grown to the desired size by reduction of $AgNO_3$. Briefly, the as-synthesized Ag seeds (15 mL, 1 mM), sodium citrate (1 mL, 80 mM), and 36 mL of ultrapure water were heated to 100 °C under reflux. $AgNO_3$ (1.8 mL, 20 mM) solution was added dropwise, every 10 min. The solution mixture was heated for another 20 min before it was cooled down to room temperature for use.

Preparation of DNA-Conjugated Metal Nanoparticles (mNPs). The double-stranded (ds)DNA-AuNPs conjugates were prepared by conjugating the thiolated single-stranded (ss) sense strand of ERE half site to the AuNPs (to form ssDNA−AuNPs) and then annealing the antisense strand with the as-prepared ssDNA−AuNPs conjugates. The ssDNA−AuNPs conjugates were prepared according to the previously published protocol.[42,43] In a typical conjugation, the deprotected thiol-modified ssDNA (final concentration of oligonucleotides is 2−3 μM) was added into the as-synthesized AuNPs solution. After aging for 24 h, the colloidal solution was brought to 0.05 M NaCl in 10 mM phosphate buffer (PB) by dropwise addition of concentrated buffer solution (1 M NaCl and 0.1 M PB), and allowed to stand for 12 h, then salted to 0.1 M NaCl and aged for another 12 h. To remove excess DNA, the particle solution was centrifuged at 11000 rpm for 30 min and the red color precipitates were resuspended in 0.1 M PBS buffer (10 mM PB and 0.1 M NaCl, pH 7.4). The washing steps were repeated three times. The final ssDNA-AuNPs conjugates were redispersed in 195 μL of DNA annealing buffer (0.1 M PBS and 0.001 M EDTA, pH 7.4), and 5 μL of unmodified cDNA (100 μM) (three bases shorter than the sense strand) was added for hybridization. The solution was heated at 90 °C for 5 min and slowly cooled down to room temperature for 30 min. Finally, the as-prepared double-stranded (ds)DNA-AuNPs conjugates (with three-base sticky ends) were redispersed in 200 μL of 0.1 M PBS buffer solution, after washing twice by centrifugation at 11000 rpm for 15 min. Similar procedure was applied for the preparation of DNA-AgNPs conjugates, except that the salt-aging process was carried out in four consecutive steps in every 6 h due to the instability of AgNPs solution.

Protein−DNA Binding Assays. The assay was performed by first mixing two sets of dsDNA−mNPs conjugates (in 0.1 M PBS) with complementary overhang (*e.g.*, v1 and v2) at a 1:1 ratio (40 μL each). A 20 μL portion of ERα in protein binding buffer (0.1 M PBS, 0.5 mM EDTA, 1 mM DTT, 5% of glycerol, and desirable amount of KCl) was then added to the 80 μL of nanoparticles mixture. The final ERα concentration in the protein−particle mixture solutions is 25, 50, 100, or 200 nM, and the final KCl concentration is either 25 or 50 mM. A series of negative control experiments were carried out by replacing complementary v1−v2 NPs mixture with either s1−s2 NPs mixture (40 μL each), as-prepared dsDNA−NPs alone (*e.g.*, v1−NPs, 80 μL), or noncomplementary v1−s1 NPs mixture (40 μL each). An irrelevant protein (*i.e.*, BSA) was also used to replace ERα as reference for sequence-specific binding assay.

Acknowledgment. X. Su would like to acknowledge the Agency for Science, Technology and Research (A*STAR), Singapore for the financial support under the grant CCOG01_005_2008. We also thank Ms Liang Jing from NUS for her help in the synthesis of silver nanoparticles.

Supporting Information Available: UV−vis spectra and TEM images of dsDNA−AuNPs conjugates, negative control experiment with BSA, and SPR determination of salt concentration effects on ERα−ERE interaction. This material is available free of charge *via* the Internet at http://pubs.acs.org.

REFERENCES AND NOTES

1. Stewart, M. E.; Anderton, C. R.; Thompson, L. B.; Maria, J.; Gray, S. K.; Rogers, J. A.; Nuzzo, R. G. Nanostructured Plasmonic Sensors. *Chem. Rev.* **2008**, *108*, 494–521.
2. Liu, J.; Cao, Z.; Lu, Y. Functional Nucleic Acid Sensors. *Chem. Rev.* **2009**, *109*, 1948–1998.
3. Zhao, W.; Brook, M. A.; Li, Y. Design of Gold Nanoparticle-Based Colorimetric Biosensing Assays. *ChemBioChem* **2008**, *9*, 2363–2371.
4. Thaxton, C. S.; Georganopoulou, D. G.; Mirkin, C. A. Gold Nanoparticle Probes for the Detection of Nucleic Acid Targets. *Clin. Chim. Acta* **2006**, *363*, 120–126.
5. Elghanian, R.; Storhoff, J. J.; Mucic, R. C.; Letsinger, R. L.; Mirkin, C. A. Selective Colorimetric Detection of Polynucleotides Based on the Distance-Dependent Optical Properties of Gold Nanoparticles. *Science* **1997**, *277*, 1078–1081.
6. Chen, S. J.; Huang, Y. F.; Huang, C. C.; Lee, K. H.; Lin, Z. H.; Chang, H. T. Colorimetric Determination of Urinary Adenosine Using Aptamer-Modified Gold Nanoparticles. *Biosens. Bioelectron.* **2008**, *23*, 1749–1753.
7. Huang, C. C.; Huang, Y. F.; Cao, Z.; Tan, W.; Chang, H. T. Aptamer-Modified Gold Nanoparticles for Colorimetric Determination of Platelet-Derived Growth Factors and Their Receptors. *Anal. Chem.* **2005**, *77*, 5735–5741.
8. Aili, D.; Selegard, R.; Baltzer, L.; Enander, K.; Liedberg, B. Colorimetric Protein Sensing by Controlled Assembly of Gold Nanoparticles Functionalized with Synthetic Receptors. *Small* **2009**, *5*, 2445–24512.
9. Guarise, C.; Pasquato, L.; Filippis, V.; Scrimin, P. Gold Nanoparticles-Based Protease Assay. *Proc. Natl. Acad. Sci. U.S.A.* **2006**, *103*, 3978–3982.
10. Slocik, J. M.; Zabinski, J. S., Jr.; D., M. Phillips; Naik, R. R. Colorimetric Response of Peptide-Functionalized Gold Nanoparticles to Metal Ions. *Small* **2008**, *4*, 548–551.
11. Lvy, R.; Thanh, N. T. K.; Doty, T. R. C.; Hussain, I.; Nichols, R. J.; Schiffrin, D. J.; Brust, M.; Fernig, D. G. Rational and Combinatorial Design of Peptide Capping Ligands for Gold Nanoparticles. *J. Am. Chem., Soc.* **2004**, *126*, 10076–10084.
12. Hirsch, L. R.; Jackson, J. B.; Lee, A.; Halas, N. J.; Wes, J. L. Whole Blood Immunoassay Using Gold Nanoshells. *Anal. Chem.* **2003**, *75*, 2377–2381.
13. Liu, X.; Dai, Q.; Austin, L.; Coutts, J.; Knowles, G.; Zou, J.; Chen, H.; Huo, Q. A One-Step Homogeneous Immunoassay for Cancer Biomarker Detection Using Gold Nanoparticle Probes Coupled with Dynamic Light Scattering. *J. Am. Chem. Soc.* **2008**, *130*, 2780–2782.
14. Neely, A.; Perry, C.; Varisli, B.; Singh, A. K.; Arbneshi, T.; Senapati, D.; Kalluri, J. R.; Ray, P. C. Ultrasensitive and Highly Selective Detection of Alzheimer's Disease Biomarker Using Two-Photon Rayleigh Scattering Properties of Gold Nanoparticle. *ACS Nano* **2009**, *3*, 2834–2840.
15. Thompson, D. G.; Enright, A.; Faulds, K.; Smith, W. E.; Graham, D. Ultrasensitive DNA Detection Using Oligonucleotide-Silver Nanoparticle Conjugates. *Anal. Chem.* **2008**, *80*, 2805–2810.
16. Liu, S. H.; Zhang, Z. H.; Han, M. Y. Gram-Scale Synthesis and Biofunctionalization of Silica-Coated Silver Nanoparticles for Fast Colorimetric DNA Detection. *Anal. Chem.* **2005**, *77*, 2595–2600.
17. Sato, K.; Hosokawa, K.; Maeda, M. Rapid Aggregation of Gold Nanoparticles Induced by Non-Cross-Linking DNA Hybridization. *J. Am. Chem. Soc.* **2003**, *125*, 8102–8103.
18. Lee, J.-S.; Ulmann, P. A.; Han, M. S.; Mirkin, C. A. A DNA-Gold Nanoparticle-Based Colorimetric Competition Assay for the Detection of Cysteine. *Nano Lett.* **2008**, *8*, 529–533.
19. Song, G.; Chen, C.; Qu, X.; Miyoshi, D.; Ren, J.; Sugimoto, N. Small-Molecule-Directed Assembly: A Gold Nanoparticle-Based Strategy for Screening of Homo-adenine DNA Duplex Binders. *Adv. Mater.* **2008**, *20*, 706–710.

20. Han, M. S.; Lytton-Jean, A. K. R.; Mirkin, C. A. A Gold Nanoparticle Based Approach for Screening Triplex DNA Binders. *J. Am. Chem. Soc.* **2006**, *128*, 4954–4955.
21. Hurst, S. J.; Han, M. S.; Lytton-Jean, A. K. R.; Mirkin, C. A. Screening the Sequence Selectivity of DNA-Binding Molecules Using a Gold Nanoparticle-Based Colorimetric Approach. *Anal. Chem.* **2007**, *79*, 7201–7205.
22. Han, M. S.; Lytton-Jean, A. K. R; Oh, B. K.; Heo, J.; Mirkin, C. A. Colorimetric Screening of DNA-Binding Molecules with Gold Nanoparticle Probes. *Angew. Chem., Int. Ed.* **2006**, *45*, 1807–1810.
23. Lee, J.-S.; Han, M. S.; Mirkin, C. A. Colorimetric Detection of Mercuric Ion (Hg^{2+}) in Aqueous Media using DNA-Functionalized Gold Nanoparticles. *Angew. Chem., Int. Ed.* **2007**, *46*, 4093–4096.
24. Liu, J.; Lu, Y. Fast Colorimetric Sensing of Adenosine and Cocaine Based on a General Sensor Design Involving Aptamers and Nanoparticles. *Angew. Chem., Int. Ed.* **2006**, *45*, 90–94.
25. Chen, S. J.; Huang, Y. F.; Huang, C. C.; Lee, K. H.; Lin, Z. H.; Chang, H. T. Colorimetric Determination of Urinary Adenosine Using Aptamer-Modified Gold Nanoparticles. *Biosens. Bioelectron.* **2008**, *23*, 1749–1753.
26. Xue, X. J.; Wang, F.; Liu, X. G. One-Step, Room Temperature, Colorimetric Detection of Mercury (Hg^{2+}) Using DNA/Nanoparticle Conjugates. *J. Am. Chem. Soc.* **2008**, *130*, 3244–3245.
27. Lee, J. H.; Wang, Z.; Liu, J.; Lu, Y. Highly Sensitive and Selective Colorimetric Sensors for Uranyl (UO_2^{2+}): Development and Comparison of Labeled and Label-free DNAzyme-Gold Nanoparticle Systems. *J. Am. Chem. Soc.* **2008**, *130*, 14217–14226.
28. Xu, X.; Han, M. S.; Mirkin, C. A. A Gold-Nanoparticle-Based Real-Time Colorimetric Screening Method for Endonuclease Activity and Inhibition. *Angew. Chem.* **2007**, *46*, 3468–3470.
29. Song, G. T.; Chen, C.; Ren, J. S.; Qu, X. G. A Simple, Universal Colorimetric Assay for Endonuclease/Methyltransferase Activity and Inhibition Based on an Enzyme-Responsive Nanoparticle System. *ACS Nano* **2009**, *3*, 1183–1189.
30. Lim, I. I. S.; Chandrachud, U.; Wang, L.; Gal, S.; Zhong, C. J. Assembly-Disassembly of DNAs and Gold Nanoparticles: A Strategy of Intervention Based on Oligonucleotides and Restriction Enzymes. *Anal. Chem.* **2008**, *80*, 6038–6044.
31. Zhao, W.; Ali, M. M.; Aguirre, S. D.; Brook, M. A.; Li, Y. Paper-Based Bioassays Using Gold Nanoparticle Colorimetric Probes. *Anal. Chem.* **2008**, *80*, 8431–8437.
32. Zhao, W. A.; Lam, J. C. F.; Chiuman, W.; Brook, M. A.; Li, Y. F. Enzymatic Cleavage of Nucleic Acids on Gold Nanoparticles: A Generic Platform for Facile Colorimetric Biosensors. *Small* **2008**, *4*, 810–816.
33. Fang, J.; Yu, L. L.; Gao, P.; Wei, Y. N. Detection of Protein−DNA Interaction and Regulation Using Gold Nanoparticles. *Anal. Biochem.* **2010**, *39*, 262–267.
34. Maye, M. M.; Nykypanchuk, D.; van der Lelie, D.; Gang, O. A Simple Method for Kinetic Control of DNA-Induced Nanoparticle Assembly. *J. Am. Chem. Soc.* **2006**, *128*, 14020–14021.
35. Kim, J. Y.; Dong, H. L.; Kim, S. J.; Jang, D. J. Preferentially Linear Connection of Gold Nanoparticles in Derivatization with Phosphorothioate Oligonucleotides. *J. Colloid Interface Sci.* **2008**, *326*, 387–391.
36. Su, X.; Lin, C.-Y.; O'Shea, S. J.; Teh, H. F.; Peh, W. Y. X.; Thomsen, J. S. Combinational Application of Surface Plasmon Resonance Spectroscopy and Quartz Crystal Microbalance for Studying Nuclear Hormone Receptor-Response Element Interactions. *Anal. Chem.* **2006**, *78*, 5552–5558.
37. Tan, Y. N.; Su, X.; Liu, E. T.; Thomsen, J. S. Gold-Nanoparticle-Based Assay for Instantaneous Detection of Nuclear Hormone Receptor-Response Elements Interactions. *Anal. Chem.* **2010**, *82*, 2759–2765.
38. Hard, T.; Lundback, T. Thermodynamics of Sequence-Specific Protein-DNA Interactions. *Biophys. Chem.* **1996**, *62*, 121–139.
39. Wei, H.; Chen, C.; Han, B.; Wang, E. Enzyme Colorimetric Assay Using Unmodified Silver Nanoparticles. *Anal. Chem.* **2008**, *80*, 7051–7055.
40. Su, X.; Kanjanawarut, R. Control of Metal Nanoparticles Aggregation and Dispersion by PNA and PNA−DNA Complexes, and Its Application for Colorimetric DNA Detection. *ACS Nano* **2009**, *3*, 2751–2759.
41. Kanjanawarut, R; Su, X. Colorimetric Detection of DNA Using Unmodified Metallic Nanoparticles and Peptide Nucleic Acid Probes. *Anal. Chem.* **2009**, *81*, 6122–6129.
42. Storhoff, J. J.; Elghanian, R.; Mirkin, C. A.; Letsinger, R. L. Sequence-Dependent Stability of DNA-Modified Gold Nanoparticles. *Langmuir* **2002**, *18*, 6666–6670.
43. Liu, J.; Lu, Y. Preparation of Aptamer-Linked Gold Nanoparticles Purple Aggregates for Colorimetric Sensing of Analytes. *Nat. Protoc.* **2006**, *1*, 246–252.